

Electronic Supplementary Information (ESI)

Self-Healing, Superhydrophobic Coating Based on Mechanized Silica Nanoparticles for Reliable Protection of Magnesium Alloy

ChenDi Ding, Ying Liu, MingDong Wang, Ting Wang, JiaJun Fu*

School of Chemical Engineering, Nanjing University of Science and Technology,
Nanjing 210094, China

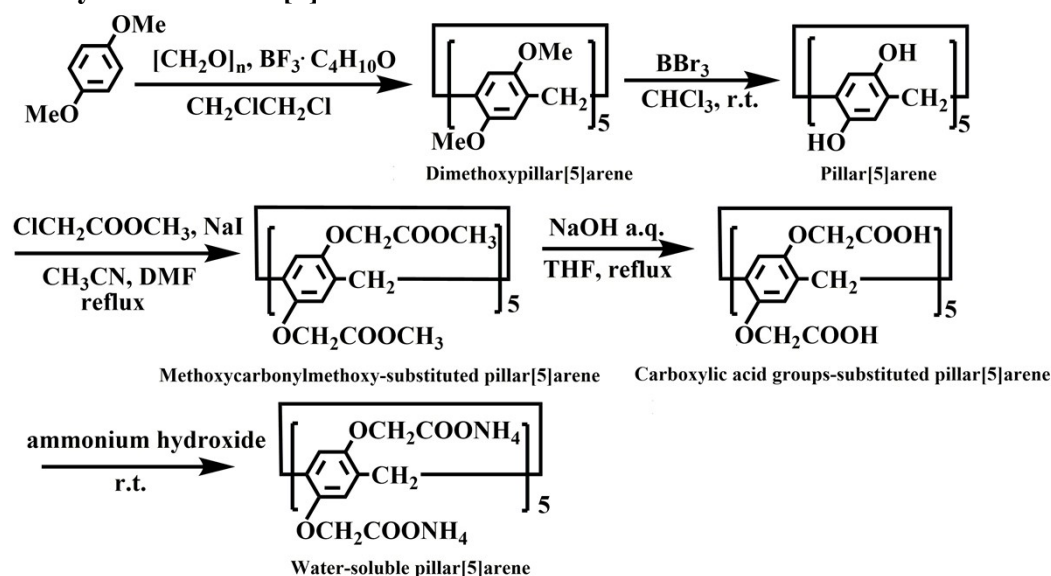
E-Mail: fujiajun668@gmail.com

Table of Contents

1	Synthesis Procedure	1
1.1	Synthesis of WP[5]	1
1.2	Synthesis of APy-HDA	3
1.3	Synthesis of principal elements for preparation of MSNPs	4
2	Preparation and Characterization of MSNs	6
3	N₂ adsorption-desorption isotherms	6
4	TG analyses	7
5	Calibration curve of HMAP and UV/Vis spectra of released HMAP	8
6	Control experiment	8
7	Cross-section SEM images	9
8	XPS characterization of MSNPs@SNAP and PFDS/MSNPs@SNAP	10
9	Potentiodynamic polarization results	10
10	Corrosion inhibition performance of HMAP	11

1 Synthesis Procedure

1.1 Synthesis of WP[5]



Dimethoxypillar[5]arene: 1,4-dimethoxybenzene (1.38 g, 10 mmol), paraformaldehyde (0.93 g, 30 mmol) was dissolved in 1,2-dichloroethane (20 mL). The mixture was stirred for 30 min at 30 °C. Then boron trifluoride diethyl etherate (1.25 mL, 10 mmol) was added. The solution color changed from light green to dark green immediately. The mixture was precipitated in methanol (40 mL) and filtered. Column chromatography (silica gel, CH₂Cl₂) afforded a white solid product (0.62 g, 0.83 mmol). Yield: 41%.

¹H NMR (CDCl₃, 300 MHz): δ (ppm) 6.80 (s, 10H), 3.80 (s, 10H), 3.68 (s, 30H).

¹³C NMR (CDCl₃, 75 MHz): δ (ppm) 150.60, 128.21, 113.78 (C of benzene ring); 55.66 (C of methoxy group); δ29.43 (C of methylene bridge)

MS (ESI): m/z calcd. for C₄₅H₅₀O₁₀: 750.34; found: 751.28 [M+H]⁺.

Pillar[5]arene: Dimethoxypillar[5]arene (2.00 g, 2.7 mmol) was dissolved in chloroform (150 mL) under ice bath. Then boron tribromide (5.13 mL, 55 mmol) was added in the mixture. The mixture was stirred at room temperature for 72 h. Afterwards, water (150 mL) was added to the reaction mixture under ice bath to quench the reaction. The resulting precipitate was filtered and recrystallized from acetone and water to yield pillar[5]arene as a white solid product (1.5g, 1.99 mmol). Yield: 92%.

¹H NMR ((CD₃)₂CO, 300 MHz): δ (ppm) 6.80 (s, 10H), 3.80 (s, 10H), 3.68 (s, 30H).

¹³C NMR (CD₃)₂CO, 75 MHz): δ (ppm) 146.21, 125.92, 116.17 (C of benzene ring); 30.55 (C of methylene bridge).

MS (ESI): m/z calcd. for C₃₅H₃₀O₁₀: 610.18; found: 609.00 [M-H]⁻.

Methoxycarbonylmethoxy-substituted pillar[5]arene: Pillar[5]arene (1.22 g, 2.0 mmol), K_2CO_3 (3.31 g, 24.0 mmol) were dissolved in 50 mL CH_3CN and 20 mL DMF. The mixture was stirred under N_2 atmosphere for 30 min. Afterwards, NaI (20.0 mg) and $ClCH_2COOCH_3$ (4.375 mL, 50mmol) were added to the reaction mixture. The solution was heated to reflux for 24 h. After cooling to the reaction temperature, the mixture was filtrated and washed thoroughly with chloroform. The filtrate was removed under vacuum. Then methanol was added to the residue to afford pale yellow solid. Column chromatography (silica gel, $CH_2Cl_2:CH_3COCH_3 = 97:3$ to $95:5$) afforded a white solid product (0.86 g, 0.65 mmol). Yield: 32%.

1H NMR ($CDCl_3$, 300 MHz): δ (ppm) 7.04 (s, 10H), 4.56 (s, 20H), 3.87 (s, 10H), 3.60 (s, 30H).

^{13}C NMR ($CDCl_3$, 75 MHz): δ (ppm) 169.74 (C of carbonyl); 148.86, 128.41, 114.41 (C of benzene ring); 65.41 (C of O-methylene); 51.65 (C of methoxy group); 29.23 (C of methylene bridge).

MS (ESI): m/z calcd. for $C_{35}H_{30}O_{10}$: 1330.40; found: 1353.69 $[M+Na]^+$.

Carboxylic acid-substituted pillar[5]arene: Methoxycarbonylmethoxy-substituted pillar[5]arene (265 mg, 0.2 mmol) was dispersed in 40 mL THF. Afterwards, 10 mL 20% aqueous sodium hydroxide was added into the reaction mixture. The solution was heated to reflux for 12 h. After cooling to room temperature, the reaction mixture was concentrated under reduced pressure. Then hydrochloric acid solution was added to acidify the mixture and afford the white solid. The product was collected by centrifugation and washed thoroughly by water to give carboxylic acid-substituted pillar[5]arene (200 mg, 0.17mmol). Yield: 85%.

1H NMR ($(CD_3)_2SO$, 300 MHz): δ (ppm) 12.96 (br, 10H), 7.10 (s, 10H), 4.71 (d, $J=9.6$ Hz, 10H), 4.40 (d, $J=9.6$ Hz, 10H), 3.74 (s, 10H).

^{13}C NMR ($(CD_3)_2SO$, 75 MHz): δ (ppm) 170.87 (C of carbonyl); 148.82, 128.38, 114.58 (C of benzene ring); 65.46 (C of O-methylene); 28.94 (C of methylene bridge).

MS (ESI): m/z calcd. for $C_{35}H_{30}O_{10}$: 1190.24; found: 1189.34 $[M-H]^-$.

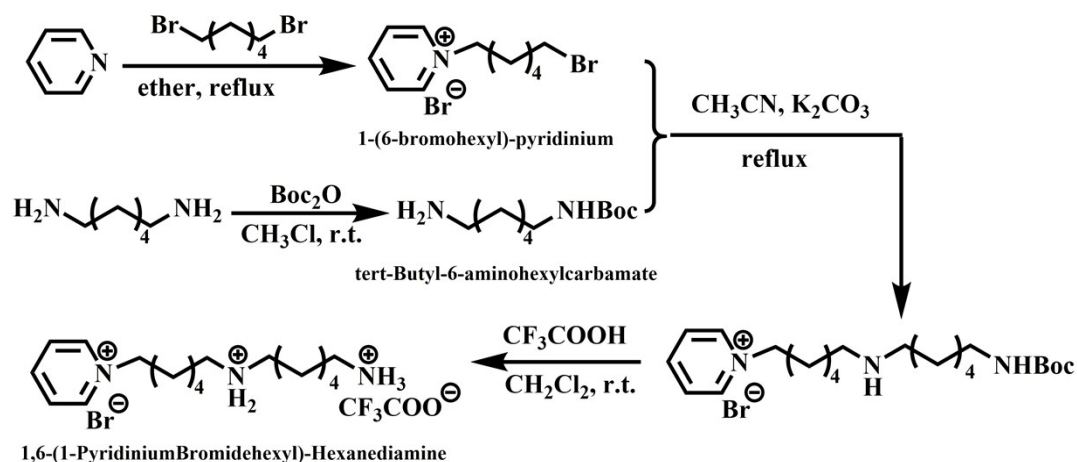
Water-soluble pillar[5]arene: Carboxylic acid-substituted pillar[5]arene (200 mg, 0.17 mmol) was dispersed in 40 mL water. Afterwards, ammonium hydroxide (30.7 mg, 1.8 mmol) was added. The mixture was stirred at room temperature for 4 h. After filtration, water was removed under reduced pressure to give water-soluble pillar[5]arene as a white solid (195 mg, 0.14 mmol). Yield: 82%.

1H NMR (D_2O , 300 MHz): δ (ppm) 6.60 (s, 10H), 4.10 (s, 20H), 4.71 (d, $J=9.8$ Hz, 10H), 3.74 (s, 10H).

^{13}C NMR (D_2O , 75 MHz): δ (ppm) 175.99 (C of carbonyl); 149.52, 129.05, 115.46 (C of benzene ring); 67.29 (C of O-methylene); 29.13 (C of methylene bridge).

MS (ESI): m/z calcd. for $C_{55}H_{80}N_{10}O_{30}$: 1360.50; found: 638.33 $[M-6Na+4H]^{2+}$.

1.2 Synthesis of APy-HDA



Scheme S2 Synthetic route of APy-HDA.

1-(6-bromohexyl)-pyridinium: 1,6-dibromohexane (9.15 g, 37.5 mmol) was dissolved in diethyl ether (12.5 mL). Pyridinium (1.0 g, 0.0126 mmol) in dry diethyl ether (2 mL) was added dropwise to the above mixture under stirring with ice bath. Afterwards, the mixture was reacted at reflux condition for 40 h. Then the solution was filtered to collect the resulting white precipitate. The white precipitate was wash with diethyl ether to give a white powder 1-(6-bromohexyl)-pyridinium (2.77 g, 68%).

1H NMR (D_2O , 300 MHz): δ (ppm) 8.737 (d, $J=5.3$ Hz, 2H), 8.429 (t, $J=7.5$ Hz, 1H), 7.953 (t, $J=6.9$ Hz, 2H), 4.506 (t, $J=7.6$ Hz, 2H), 3.369 (t, $J=6.3$ Hz, 2H), 1.926 (q, $J=7.5$ Hz, 2H), 1.727 (q, $J=6.8$ Hz, 2H), 1.367 (q, $J=7.7$ Hz, 2H), 1.251 (q, $J=7.5$ Hz, 2H).

^{13}C NMR (D_2O , 75 MHz): δ (ppm) 23.32, 25.76, 29.29, 30.19, 34.09, 60.17, 126.88, 143.59, 145.92.

Tert-butyl-6-aminohexylcarbamate: 1,6-hexanediamine (6 g, 0.05 mol) was dissolved in chloroform (200 mL) and stirred for 30 min. A solution of di-tert-butyl dicarbonate (2.2 g, 10 mmol) in chloroform (20 mL) was added dropwise to 1,6-hexanediamine solution with ice-bath over a 24 h period. The reaction mixture was stirred for three days at room temperature, filtered and concentrated. Then the residue was dissolved in 200 mL ethyl acetate and wash with half-saturated NaCl solution (300 mL) for three times. The organic was separated and dried with sodium sulfate. The ethyl acetate was removed under vacuum. The product was used in the next step without further purification.

1H NMR ($CDCl_3$, 300 MHz): δ (ppm) 4.70 (s, 1H), 3.01 (q, $J=6.7$ Hz, 2H), 2.58 (t, $J=6.6$ Hz, 2H), 1.39 (m, 13H), 1.19 (m, 4 H) ppm.

¹³C NMR (CDCl₃, 75 MHz): δ (ppm) 155.8, 78.0, 42.5, 41.3, 32.9, 30.4, 28.8, 26.5, 26.2.

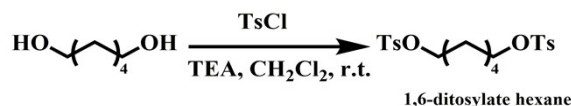
1,6-(1-pyridiniumbromidehexyl)-hexanediamine: Tert-butyl-6-aminohexyl carbamate (3.76 g, 17.0 mmol), K₂CO₃ (3.31 g, 24 mmol) were dissolved in acetonitrile (30 mL) at 50°C. Afterwards, 1-(6-bromohexyl)-pyridinium (0.413 g, 1.28 mmol) in acetonitrile (20 mL) was added dropwise into the reaction mixture under stirring. After reacting for 12 h, the mixture was concentrated under vacuum to afford brown oily intermediate compound and then it was purified by extraction with chloroform and water. The aqueous phase was isolated and concentrated under vacuum. The residual was dissolved in CH₂Cl₂ (6 mL). 1:1 TFA/CH₂Cl₂ (12 mL) was added dropwise with ice bath. The reaction was allowed to stand for 2 h at room temperature. The solution was concentrated, and the resulting residue was recrystallized from ethanol/ethyl acetate and dried under vacuum to obtain 1,6-(1-pyridiniumbromidehexyl)-hexanediamine (0.338 g, 0.72 mmol). Yield: 55%.

¹H NMR (D₂O, 300MHz): δ (ppm) 8.72 (d, *J*=3.0 Hz, 2H), 8.43 (t, *J*=9.0Hz, 1H), 7.95 (t, *J*=7.5Hz, 2H), 4.50 (t, *J*=7.5Hz, 2H), 2.89 (t, *J*=3.0 Hz, 4H), 1.88 (t, *J*=9.0 Hz, 2H), 1.56 (m, 8H), 1.29 (m, 8H).

¹³C NMR (D₂O, 75 MHz): δ (ppm) 145.45, 144.02, 128.09, 61.60, 47.20, 39.19, 30.16 26.34, 24.95, 24.67.

MS (ESI): m/z calcd. for C₁₇H₃₂N₃: 278.26; found: 278.19 [M]⁺.

1.3 Synthesis of principal elements for preparation of MSNPs

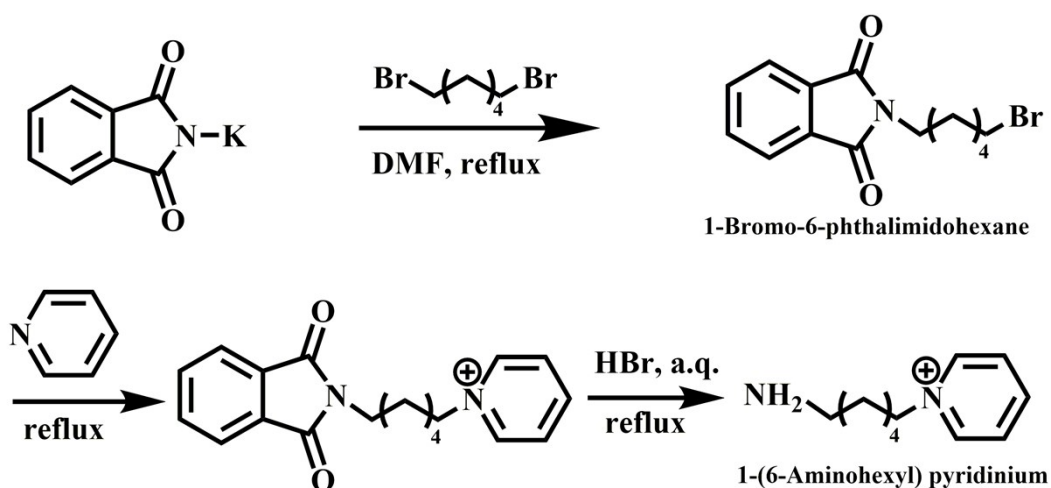


Scheme S3 Synthetic route of 1,6-ditosylate hexane.

1,6-ditosylate hexane: To a solution of 1,6-hexanediol (1.18 g, 9.99 mmol), triethylamine (6.93 mL, 50.0 mmol) and 4-dimethylaminopyridine (0.01 g, 0.08 mmol) in 20 mL of dry CH₂Cl₂. Tosyl chloride (4.75 g, 11.15 mmol) in CH₂Cl₂ (20 mL) was added dropwise under stirring with ice bath. The mixture was stirred at low temperature (~5 °C) for 1 h and at 25°C for another 12 h. The solvent was removed by reduced pressure distillation. Column chromatography (silica gel, petroleum ether: CH₂Cl₂=3:2 to 1:2) afforded a white solid (1.52 g, 3.56 mmol). Yield: 35.7%.

¹H NMR (300 MHz, CDCl₃): δ (ppm) 7.78 (d, *J*=7.7 Hz, 4H), 7.34 (d, *J*=7.9 Hz, 4H), 3.99 (t, *J*=6.0 Hz, 4H), 2.45 (s, 6H), 1.60 (m, 4H), 1.26 (m, 4H).

¹³C NMR (75 MHz, CDCl₃): δ (ppm) 144.41, 140.32, 129.78, 127.79, 70.17, 28.51, 24.68, 21.54.



Scheme S4 Synthetic route of 1-(6-aminohexyl)-pyridinium.

1-bromo-6-phthalimido-hexane: 1,6-dibromohexane (12.25 g, 50 mmol) and potassium phthalimide (1.86 g, 10 mmol) were dissolved in DMF (10 ml). The resulting solution was stirred at 90 °C for 12 h under N₂ atmosphere. After the mixture was cooled to room temperature, the solvent was removed by reduced pressure distillation. Column chromatography (silica gel, petroleum ether:EtOAc=1:40) afforded a white solid (2.86 g, 9 mmol). Yield: 92%.

¹H NMR (300 MHz, CDCl₃): δ (ppm) 7.83 (d, 2H), 7.71 (d, 2H), 3.53 (t, *J*=7.3 Hz, 2H), 3.41 (t, *J*=6.4 Hz, 2H), 1.88 (m, 2H), 1.70 (m, 2H), 1.40 (m, 4H).

1-(6-aminohexyl)-pyridinium: A solution of 1-bromo-6-phthalimido-hexane (4.59 g, 14.8 mmol) in dry pyridine (10 mL) was heated to reflux for 4 h. After cooling to room temperature, the product was isolated and washed with diethyl ether. The product without further purification was dissolved in 25 mL of 48% HBr solution and heated to reflux for 2 h. The mixture was cooled in an ice bath, and the precipitate was removed by filtration. The aqueous filtrate was concentrated under vacuum and isopropyl alcohol was added dropwise. The title compound 1-(6-aminohexyl)pyridinium bromide hydrobromide was obtained (2.5 g, 9.69 mmol), yield: 65%.

¹H NMR (300 MHz, D₂O): δ (ppm) 8.67 (d, *J*=5.7 Hz, 2H), 8.36 (t, *J*=6.7 Hz, 1H), 7.88 (t, *J*=7.0 Hz, 2H), 4.44 (t, *J*=7.2 Hz, 2H), 2.79 (t, *J*=5.9 Hz, 2H), 1.88 (m, 2H), 1.47 (m, 2H), 1.24 (m, 4H).

¹³C NMR (75 MHz, D₂O): δ (ppm) 145.47, 144.11, 128.12, 61.65, 39.20, 30.19, 26.36, 24.96, 24.68.

MS (ESI): *m/z* calcd. for C₁₁H₁₉N₂: 179.15; found: 179.12 [M]⁺.

2 Preparation and Characterization of MSNs

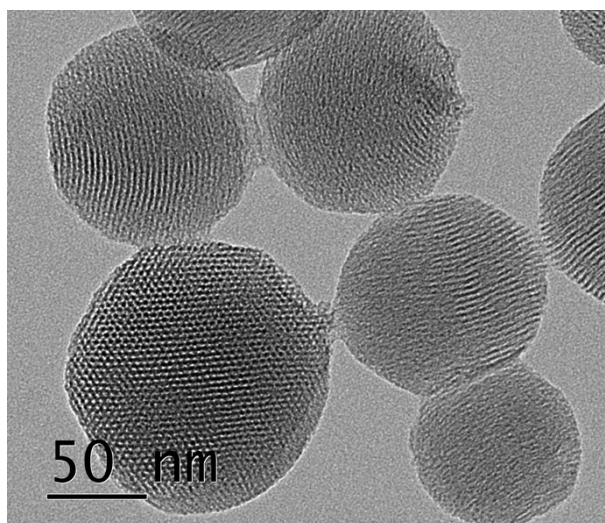


Fig. S1 TEM of MSNs.

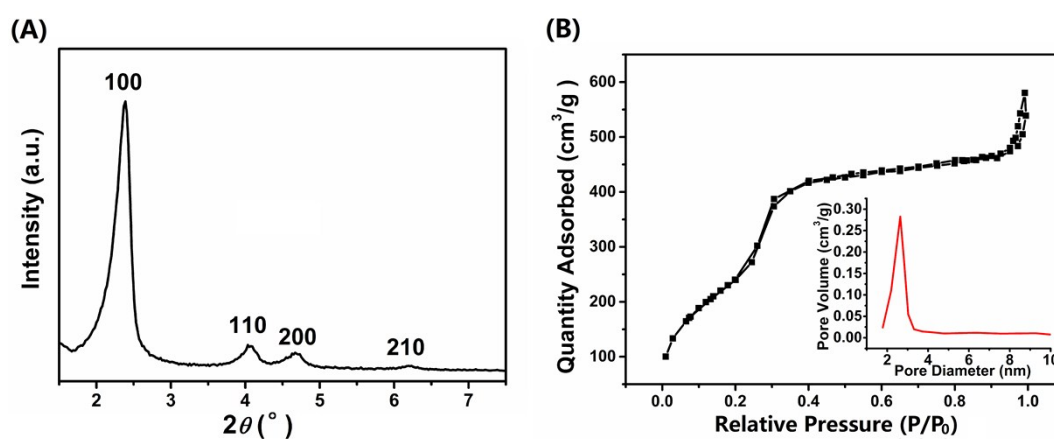


Fig. S2 (A) SA-XRD pattern and (B) N_2 adsorption-desorption isotherm and pore size distribution of MSNs.

3 N_2 adsorption-desorption isotherms

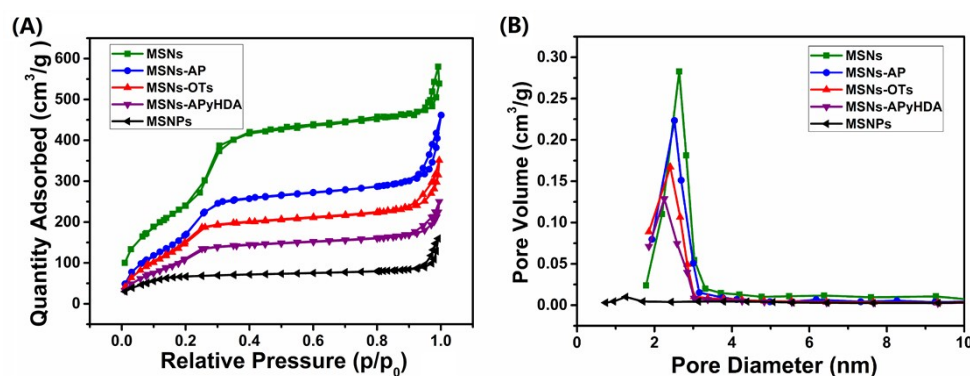


Fig. S3 (A) N_2 adsorption-desorption isotherms and (B) pore size distributions of MSNs, MSNs-AP, MSNs-OTs, MSNs-APyHDA and MSNPs.

Table S1 Physicochemical properties of MSNs, MSNs-AP, MSNs-OTs, MSNs-APyHDA and MSNPs.

Materials	Specific surface area ($\text{m}^2 \text{g}^{-1}$)	Pore size (nm)	Total pore volume ($\text{cm}^3 \text{g}^{-1}$)
MSNs	1135.4	2.64	0.89
MSNs-AP	886.2	2.52	0.78
MSNs-OTs	720.6	2.41	0.65
MSNs-APyHDA	438.5	2.25	0.51
MSNPs	135.7	--	0.12

4 TG analyses

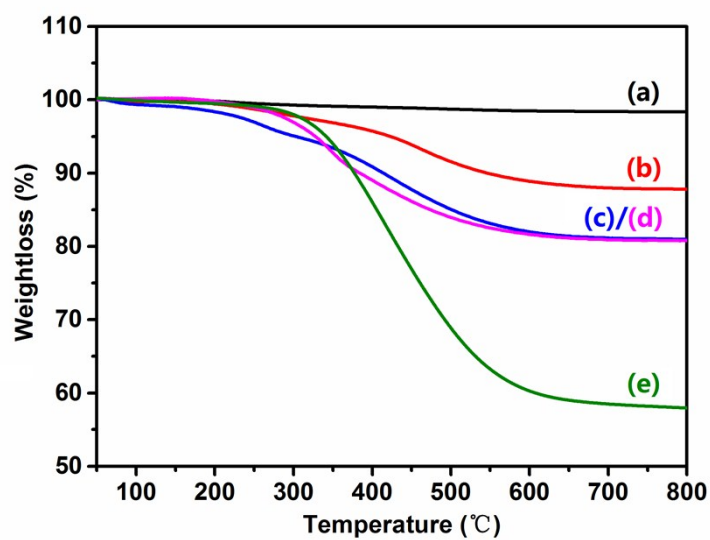


Fig. S4 TG analyses of (a) MSNs, (b) MSNs-AP, (c) MSNs-OTs, (d) MSNs-APyHDA and (e) MSNPs.

5 Calibration curve of HMAP and UV/Vis spectra of released HMAP

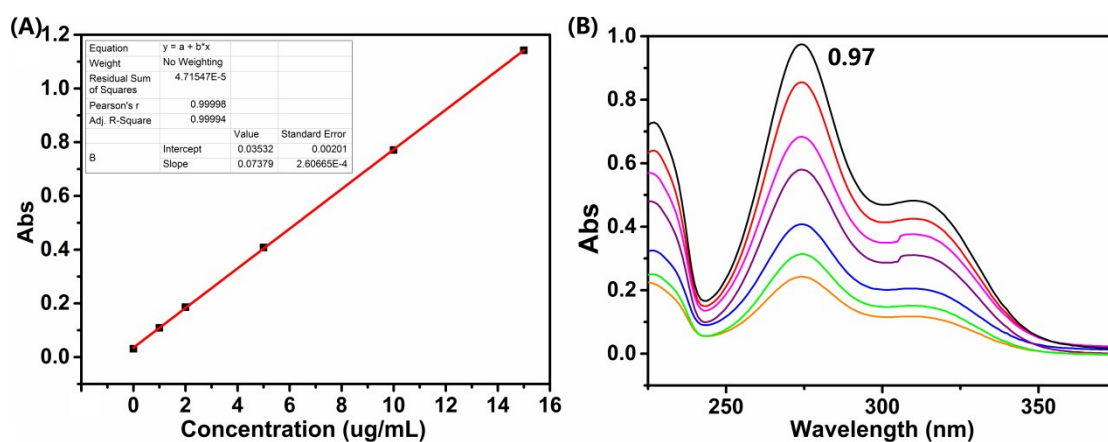
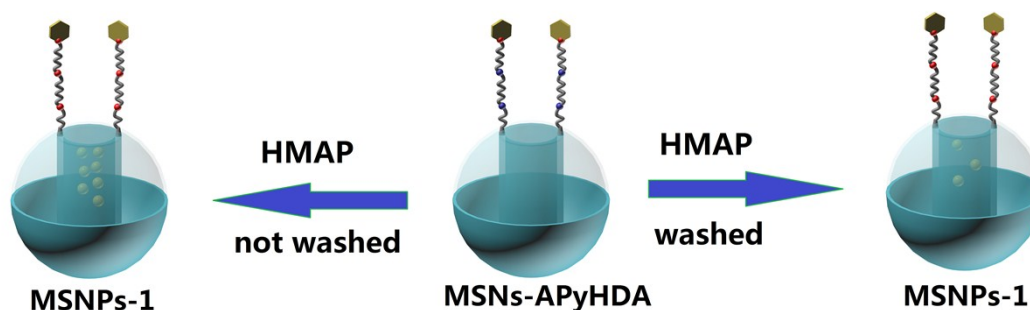


Fig. S5 (A) Calibration curve of UV/Vis absorption intensity of HMAP. (B) The UV/Vis absorption spectra of HMAP released from MSNPs completely (black line); under pH 12.0 for 6.5 h (red line); under pH 10.0 for 6.5 h (pink line); under pH 8.0 for 6.5 h (green line) and under 2.0 mM Mg^{2+} for 6.5 h (purple line); under 0.2 mM Mg^{2+} for 6.5 h (blue line) and under 0.02 mM Mg^{2+} for 6.5 h (yellow line).

6 Control experiment



Scheme S5 Schematic diagram of control experiment.

MSNPs-1 were assembled to conduct the control experiment. The synthetic procedure of MSNPs-1 was as the same as that for MSNPs, except for the lack of WP[5] capping procedure. The primary aim of control experiment is to confirm the gatekeeper role of WP[5].

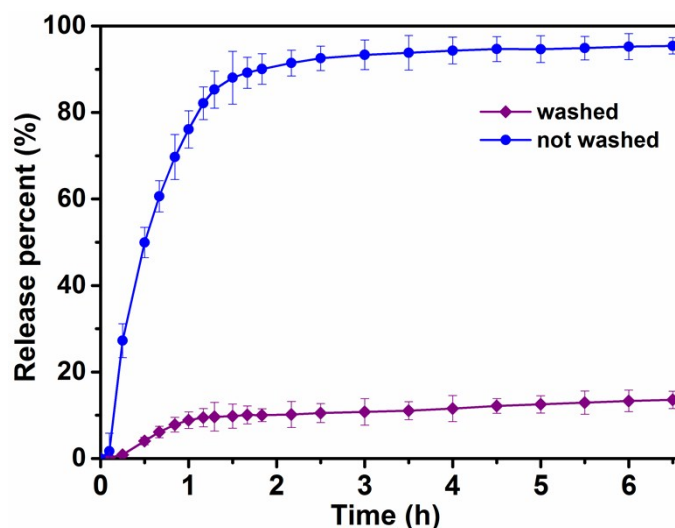


Fig. S6 The release profiles of HMAP from MSNPs-1 under neutral solution.

As illustrated in Fig. S6, if MSNPs-1 were thoroughly washed to remove the HMAP physically adsorbed on surface of MSNs, only a very slight amount of HMAP was released from MSNPs-1. It could be inferred that without WP[5] encircled on the functional stalks, the blocking effect disappeared and the majority of HMAP was leaked from MSNPs during rinsing process. In the other case, if MSNPs-1 were not thoroughly washed, the sustained release of HMAP from MSNPs-1 in the neutral solution was observed. The addition of Mg^{2+} or alkali had little impact on the release rate of HMAP. Similarly, HMAP was only released *via* diffusion process. Overall, the lack of WP[5] makes MSNPs lose zero premature leakage and Mg^{2+} /alkali dual stimuli-responsive controlled release characteristics.

7 Cross-section SEM images

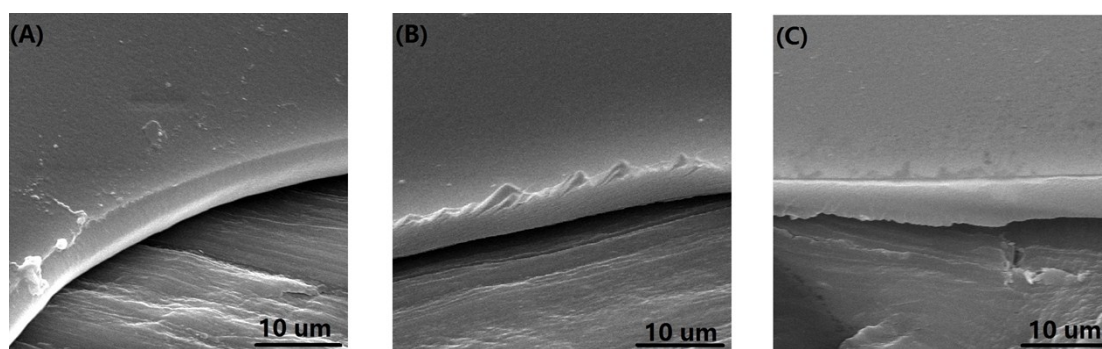


Fig. S7 Cross-section SEM images of (A) SNAP coating, (B) MSNPs@SNAP coating and (C) PFDS/MSNPs@SNAP coating.

8 XPS characterization of MSNPs@SNAP and PFDS/MSNPs@SNAP

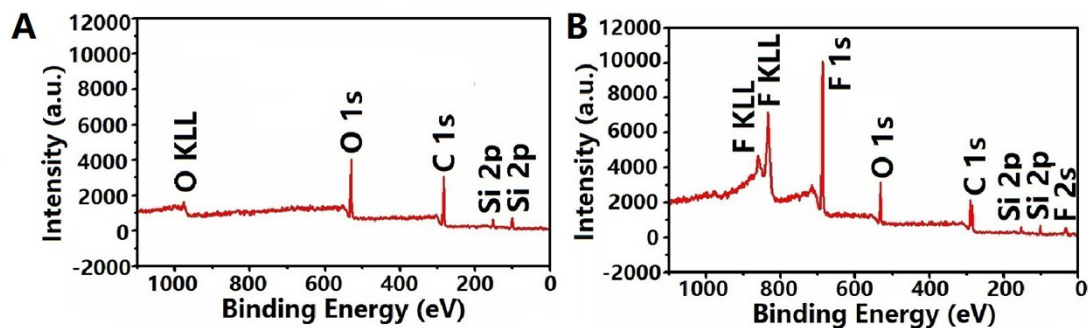


Fig. S8 XPS spectra of MSNPs@SNAP (A) and PFDS/MSNPs@SNAP (B).

9 Potentiodynamic polarization results

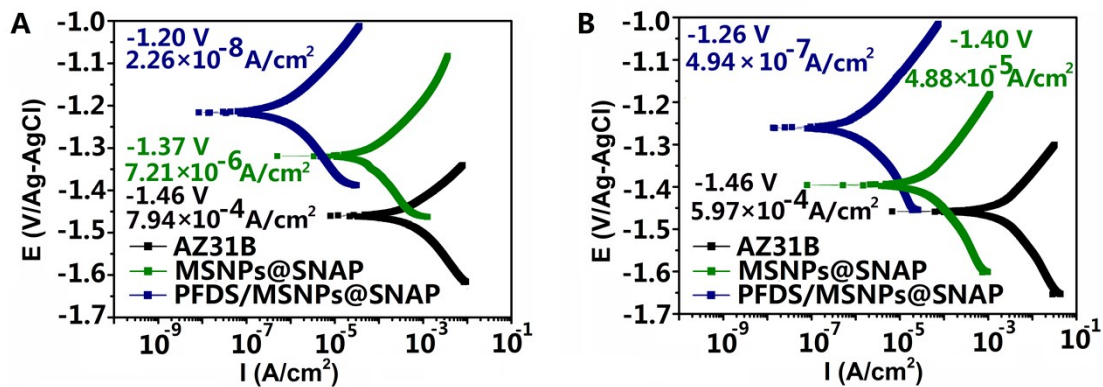


Fig. S9 Potentiodynamic polarization curves of AZ31B, MSNPs@SNAP coating and PFDS/MSNPs@SNAP coating after immersion for 30 min (A) and 7 days (B).

10 Corrosion inhibition performance of HMAP

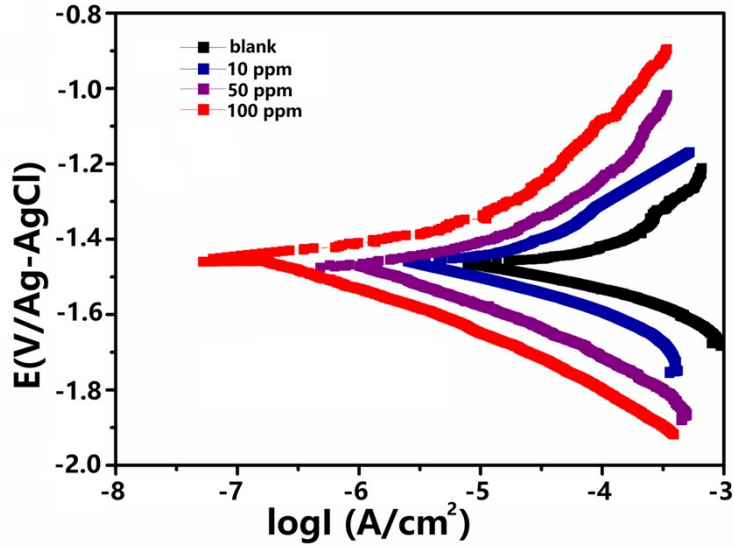


Fig. S10 Tafel polarization curves for AZ31B in 1.0 M NaCl solution without and with different concentrations of HMAP at 25°C.

Tafel polarization technique was applied to investigate the mechanisms and kinetics of anodic and cathodic reactions occurring in the metal surface. The Tafel polarization curves for AZ31B in the absence and presence of the HMAP in 1.0 M NaCl are shown in Fig. S8. The electrochemical parameters including corrosion current density (I_{corr}), open circuit potential (E_{corr}), and the inhibition efficiency (η , %) are given in Table S2. The inhibition efficiency is calculated by using the following equation:

$$\eta\% = \left(1 - \frac{I_{\text{corr},0}}{I_{\text{corr}}}\right) \times 100$$

Where $I_{\text{corr},0}$ and I_{corr} are the corrosion current densities of AZ31B immersed in 1.0 M NaCl solution with and without corrosion inhibitor, respectively.

After analysis of Tafel polarization curves, several conclusions can be drawn as following.

- (1) Upon addition of HMAP, both anodic and cathodic Tafel polarization curves shifted towards lower current density. As increasing the concentration of HMAP, the I_{corr} values decreased significantly and the η values increased obviously, implying the formation of protective film on AZ31B surface.
- (2) The presence of HMAP shifted E_{corr} values slightly compared to the uninhibited curve (blank), the largest displacement of E_{corr} observed at concentration of 100 ppm is 2.0 mV, which is far lower than the 85 mV. Generally speaking, if the displacement in corrosion potential is more than 85 mV with respect to corrosion potential of the blank, the inhibitor can be regarded as cathodic or anodic type. Therefore, HMAP is the mixed-type corrosion inhibitor.

Table S2. Tafel polarization parameters for the corrosion AZ31B in 1.0 M NaCl solution containing different concentrations of HMAP at 25 °C.

Inhibitor	Conc. (ppm)	I_{corr} ($\mu\text{A cm}^{-2}$)	E_{corr} (V)	η (%)
	blank	79.4	-1.441	-
HMAP	10	1.61	-1.441	96.71
	50	0.51	-1.441	99.36
	100	0.063	-1.439	99.92

Quantum chemical calculation was conducted with Gaussian 03 program. All electron calculations of inhibition molecule, HMAP was accomplished using the functional hybrid B3LYP density function theory (DFT), which is considered to be a standard method for modeling many chemical process, formalism with electron basis set 6-31G(d,p) for all atoms to produce highly accurate results of the molecular structure. Geometry optimizations were performed with no symmetry constraints, frequency calculation was executed simultaneously, and no imaginary frequency was found, confirming the minimum-energy structures. The following quantum chemical parameters, the energy of the highest occupied molecular orbital (E_{HOMO}) and the energy of the lowest unoccupied molecular orbital (E_{LUMO}), the energy band gap ($\Delta E = E_{LUMO} - E_{HOMO}$), dipole moment (D), molecular volume (MV) and total energy (TE) are listed in Table S3. According to the frontier molecular orbital theory, HMAP owing the high E_{HOMO} value and the low E_{LUMO} value demonstrates the high chemical reactivity, which facilitates adsorption process and thus favors good inhibition efficiency.

Table S3. The calculated quantum parameters for HMAP.

Inhibitor	E_{HOMO} (eV)	E_{LUMO} (eV)	ΔE (eV)	Dipole (D)	MV ($\text{cm}^3 \text{mol}^{-1}$)	TE (a.u.)
HMAP	-6.437	-1.62	4.817	3.6998	134.19	-574.68

Fukui indices were used to analyze the active sites accounting for donating or accepting electrons. In the present work, the condensed Fukui functions are calculated by applying finite difference approximation:

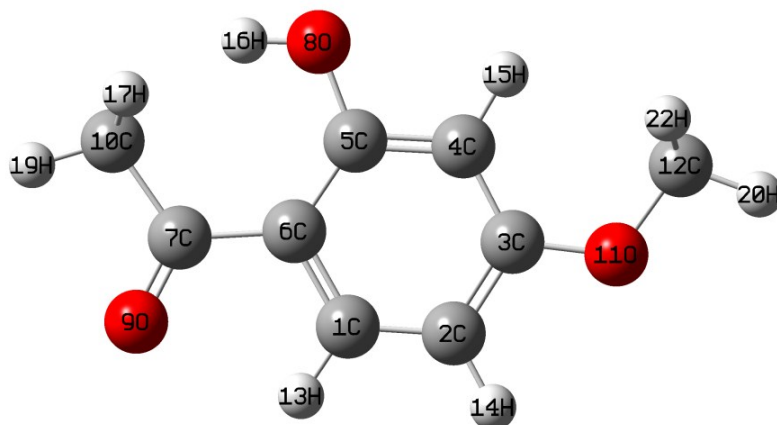
$$f_k^- = q_k(N) - q_k(N-1) \quad (\text{for electrophilic attack})$$

$$f_k^+ = q_k(N+1) - q_k(N) \quad (\text{for nucleophilic attack})$$

Fig. S9 shows the optimized geometry, and Fukui function distributions of HMAP. It can be easily seen that C2, C6 and O10 with the highest f_k^- values represent the preferred sites for donating electrons, while C1, C7 and O9 with highest f_k^+ values suggest the active sites for accepting electrons. Therefore, HMAP will adsorb on metallic surface in neutral solution mainly *via* the phenyl group and oxygen atoms in

molecular structure.

(A)



(B)

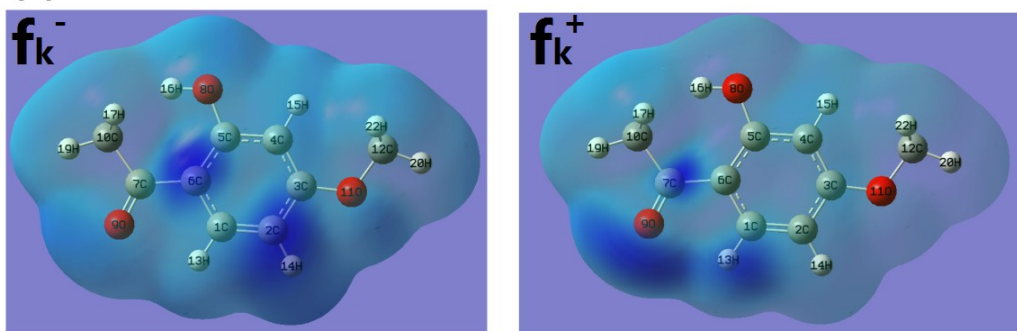


Fig. S11 (A) The optimized geometry and (B) the Fukui function of HMAP.